Journal of Solid State Chemistry **146,** 217–225 (1999)
Article ID jssc.1999.8339, available online at http://www.idealibrary.com on IDEAL®

Synthesis and Structures of New Layered Ternary Manganese Selenides: AMnSe$_2$ (A = Li, Na, K, Rb, Cs) and Na$_2$Mn$_2$Se$_3$

Joonyeong Kim and Timothy Hughbanks[1]

Department of Chemistry, Texas A&M University, P.O. Box 30012, College Station, Texas 77842-3012

Received December 31, 1998; in revised form April 7, 1999; accepted April 21, 1999

The synthesis and crystal structures of new ternary manganese selenides, AMnSe$_2$ (A = Li, Na, K, Rb, Cs) and Na$_2$Mn$_2$Se$_3$, are reported. These compounds were synthesized by solid state reaction and cation exchange techniques. The single-crystal structures of AMnSe$_2$ (A = Li, Na, Rb) and Na$_2$Mn$_2$Se$_3$ have been determined; LiMnSe$_2$: a = 4.1905(3) Å, c = 6.619(2) Å, and $P3m1$ (No. 156, Z = 1); NaMnSe$_2$: a = 4.2330(7) Å, c = 6.942(3) Å, and $P3m1$ (No. 156, Z = 1); RbMnSe$_2$: a = 4.2660(4) Å, c = 14.033(2) Å, and $I\bar{4}m2$ (No. 119, Z = 2); Na$_2$Mn$_2$Se$_3$: a = 15.689(2) Å, b = 13.888(2) Å, c = 7.220(1) Å, β = 115.65(2)°, and $C2/c$ (No. 15, Z = 8). The fundamental building blocks of the title compounds are MnSe$_4$ tetrahedra. AMnSe$_2$ (A = Li, Na) are layered compounds in which MnSe$_4$ tetrahedra share three corners in the formation of polar $^2_\infty$[MnSe$_{3/3}$Se]$^-$ layers. AMnSe$_2$ (A = K, Rb, Cs) exhibit $^2_\infty$[MnSe$_{4/2}$]$^-$ layers which are built up by four-corner-shared MnSe$_4$ tetrahedra. Na$_2$Mn$_2$Se$_3$ shows four-membered zigzag chains formed by edge-shared MnSe$_4$ tetrahedra. These chains are fused by the remaining apices to form a two-dimensional layer, $^2_\infty$[MnSe$_{2/3}$Se$_{1/3}$Se$_{1/2}$]$^-$. Magnetic susceptibility data for these compounds were fit with a modified Curie–Weiss expression. © 1999 Academic Press

Key Words: **ternary manganese selenides; solid state synthesis; crystal structures; layered compounds; magnetic susceptibilities.**

INTRODUCTION

Recent investigations of ternary manganese chalcogenides with A–Mn–Q (A = alkali metal; Q = chalcogen) compositions have revealed many new compounds with a variety of structures and magnetic properties (1–7). These ternary manganese chalcogenides are found with different compositions and distinct structures, as illustrated in Fig. 1; A_2MnQ_2 (A = K, Rb, Cs), A_6MnQ_4 (A = Na, K), A_2Mn$_3Q_4$ (A = Rb, Cs), and Na$_2$Mn$_2$S$_3$. In the first of these structure classes, one-dimensional chains, $^1_\infty$[MnQ_2]$^{2-}$, built up by edge sharing of MnQ_4 tetrahedra are found. Discrete MnQ_4^{6-} tetrahedra are found in the second structure class. The third series of compounds possess layered structures with the manganese chalcogenide framework, $^2_\infty$[Mn$_3Q_4$]$^{2-}$. The last compound also has two-dimensional layers, $^2_\infty$[Mn$_2$S$_3$]$^{2-}$, in which tetrahedra share edges and vertices to form zigzag chains that fuse into layers.

Our research on these systems originated with the discovery of the layered compounds, AMnTe$_2$ (A = Li, Na) (8, 9). These compounds exhibit polar $^2_\infty$[MnTe$_{3/3}$Te]$^{2-}$ layers, in which MnTe$_4$ tetrahedra share three corners. Our subsequent systematic survey of A–Mn–Te systems (A = alkali metals)—an effort aimed at finding other polar compounds—resulted in the synthesis of several new ternary tellurides, AMnTe$_2$ (A = K, Rb, Cs), Na$_3$Mn$_4$Te$_6$, and NaMn$_{1.56}$Te$_2$(10).

These new layered compounds, AMnTe$_2$ (A = Li, Na), crystallizing in the noncentrosymmetric space group, $P3m1$ (No. 156), are of great interest because of potential applications for the nonlinear optical (NLO) devices (11–16). Layered compounds with noncentrosymmetric structures might provide opportunities for the preparation of organic–inorganic hybrid nonlinear optical nanocomposites because they offer noncentrosymmetric environments between the layers for the guest chromophores (17–21).

Our efforts to find polar layered compounds in a A–Mn–Se system (A = alkali metals) continued and revealed new ternary selenides, AMnSe$_2$ (A = Li, Na, K, Rb, Cs), and Na$_2$Mn$_2$Se$_3$. In this paper, we report the synthesis and structures of these new ternary selenides.

EXPERIMENTAL

Materials and Instrumentation

Some compounds described herein are sensitive to both oxygen and moisture, and experimental operations were carried out under an inert gas atmosphere. Elemental starting materials were used as received. LiCl (>99.0%, Aldrich), NaCl (>99.0%, Aldrich), KCl (>99.0%, Aldrich), RbCl (>99.0%, Aldrich), and CsCl (>99.0%, Aldrich) were

[1] To whom correspondence should be addressed. Fax: (409) 847-8860. E-mail: trh@mail.chem.tamu.edu.

0022-4596/99 $30.00

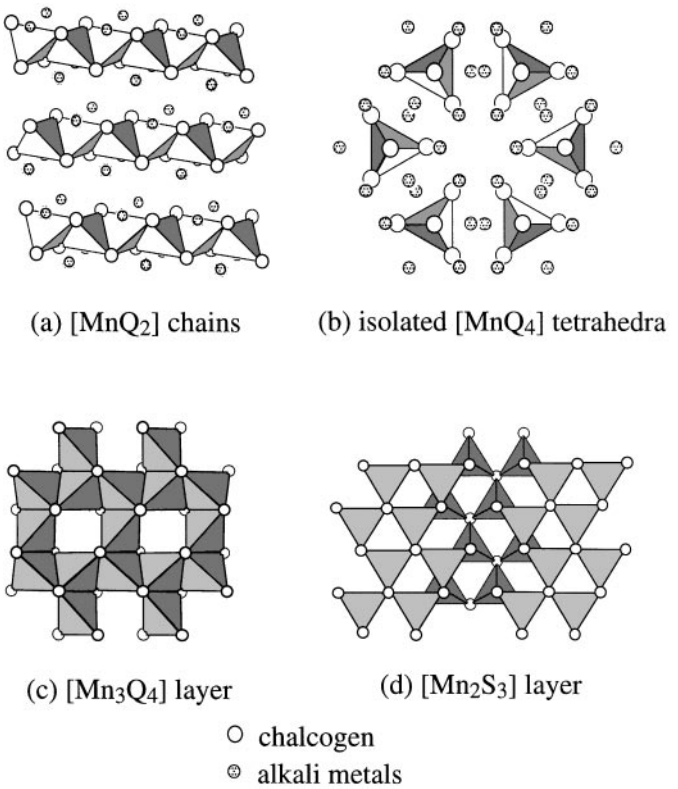

FIG. 1. (a) One-dimensional chains in A_2MnQ_2 (A = K, Rb, Cs; Q = chalcogen). (b) Isolated MnQ_4 tetrahedra in A_6MnQ_4 (A = Na, K; Q = chalcogen). (c) Layers in $A_2Mn_3Q_4$ (A = Rb, Cs; Q = chalcogen). (d) Layers in $Na_2Mn_2S_3$. White open circles are chalcogen atoms; gray small circles are alkali metals in (a) and (b).

sublimed at least twice before use. Li_2Se, Na_2Se, and K_2Se were synthesized in liquid NH_3 as described in the literature (22, 23), and MnSe was synthesized by direct reaction (24). Purity of these binary chalcogenide starting materials was confirmed by examination of Guinier X-ray powder patterns. Unless otherwise indicated, reactions were performed by the use of Nb tubes that were in turn sealed in evacuated ($\sim 10^{-4}$ Torr) silica tubes. Atomic absorption (AA) measurements were performed on a Varian SpectrAA 250 Plus instrument after dissolution of products in 20% (w/w) nitric acid. Wavelength-dispersive X-ray spectrometry (WDS) analyses were performed using a Cameca SX 50 electron microprobe equipped with four WDS spectrometers. Each spectrometer contains an X-ray diffraction crystal as a monochromator and a gas-flow proportional ionization detector. For each element analyzed, a well-characterized compound or pure element is used as a standard. Crystals of ternary selenides were collected and mounted on the top of sample holders with double-sided carbon tape. For each compound, measurements were performed at least three times for independent crystals and analyses were processed through the Cameca PAP full-quantitative matrix correction program. Temperature-dependent magnetic susceptibilities were measured with a LakeShore 7229 AC susceptometer with an external field strength of 10 Oe and ac frequency of 125 Hz over the temperature range 4–300 K. For each compound, about 50 mg was tightly sealed into a delrin sample holder. Before measurements were begun, samples were cooled to about 4 K without application of an external field and measurements were taken at 3° intervals as the temperature was increased. Data were corrected for the diamagnetic contributions of the atomic cores (25) and the sample holder.

Synthesis

$LiMnSe_2$ can be synthesized by mixing Li, MnSe, and Se in a 1:1:1 molar ratio. The temperature of the reaction vessel was uniformly raised to 230°C over 10 h, maintained at 230°C for 2 days, uniformly increased to 1000°C over 4 days, held at that temperature for 10 days, slowly cooled to 950°C at a rate of 2°C/h, and rapidly quenched to room temperature in a water bath. Orange crystals suitable for X-ray studies were found. WDS analyses of selected crystals showed Mn:Se = 1.12(3):2 and no other elements heavier than Na. AA analyses yielded the composition $Li_{0.97(2)}Mn_{0.98(1)}Se_2$.

$AMnSe_2$ (A = Na, K, Rb, Cs) compounds were synthesized by mixing $LiMnSe_2$, LiCl, and ACl in 1:2:2 mole ratios. In each case, the temperature was uniformly raised from room temperature to 850°C over 4 days, held at that temperature for 200 h, then cooled to room temperature at a rate of 2°C/h. All products contained orange-red single crystals suitable for X-ray crystallography. Alkali metal salts were removed by washing with deoxygenated water and rinsing with acetone two or three times under a nitrogen atmosphere. WDS analyses on selected crystals gave the compositions $Na_{0.93(1)}Mn_{1.09(3)}Se_2$, $K_{0.93(1)}Mn_{1.09(3)}Se_2$, $Rb_{0.91(1)}Mn_{1.05(1)}Se_2$, and $Cs_{0.88(1)}Mn_{1.04(1)}Se_2$. No other elements heavier than Na were found. AA measurements were carried out to independently determine compositions and yielded the following results: $Na_{0.97(1)}Mn_{1.08(3)}Se_2$, $K_{0.97(1)}Mn_{1.08(3)}Se_2$, $Rb_{0.98(1)}Mn_{1.01(1)}Se_2$, and $Cs_{1.00(1)}Mn_{0.94(1)}Se_2$. No lithium was detected in AA analyses.

$Na_2Mn_2Se_3$ was synthesized directly using Na, MnSe, and Se combined in a 2:2:1 ratio. The temperature of the reaction vessel was uniformly raised to 230°C over 1 day, maintained at 230°C for 2 days, uniformly increased to 850°C over 4 days, and then held at that temperature for 10 days. The reaction vessel was then cooled to room temperature at a rate of 2°C/h. Orange-red crystals of $Na_2Mn_2Se_3$ suitable for X-ray crystallography were found. WDS and AA measurements on selected crystals from the product of $Na_2Mn_2Se_3$ showed approximate compositions, $Na_{1.90(3)}Mn_{1.95(2)}Se_3$ and $Na_{2.01(1)}Mn_{2.04(1)}Se_3$, respectively. No other elements heavier than Na were found.

X-Ray Crystallography

X-ray diffraction data for $LiMnSe_2$, $NaMnSe_2$, $RbMnSe_2$, and $Na_2Mn_2Se_3$ were collected on a Siemens R3m/V diffractometer with graphite monochromated Mo$K\alpha$ radiation ($\lambda = 0.71073$ Å) at 20°C. For each compound, cell constants and an orientation matrix were obtained from a least-squares refinement using the setting angles from at least 15 centered reflections. This cell was refined by centering on at least 24 reflections in the range $15 \leq 2\theta \leq 40^\circ$. Intensity data for these compounds were collected by use of θ–2θ scans, and three check reflections monitored every 97 reflections throughout the data collection process showed no significant trends. The data were corrected for absorption using the ψ-scan technique based on 5 reflections. Structure refinements of these compounds were based on F^2 with the use of the SHELX-93 program (26).

An orange crystal of $LiMnSe_2$ having approximate dimensions $0.13 \times 0.10 \times 0.05$ mm was mounted in a glass capillary. A full sphere of the data with $5 \leq 2\theta \leq 55^\circ$ was collected ($\pm h, \pm k, \pm l$). Of the reflections, 115 were unique and 113 with $I > 2\sigma(I)$ were used in the refinements. No systematic absences were observed. Guinier X-ray diffraction data and compositional analysis had made it clear that $LiMnSe_2$ is isostructural with the known phase $LiMnTe_2$ (9), so the atomic positions of $LiMnTe_2$ were used to begin refinement.

Isotropic refinement of the structure with Mn and Se positions fully occupied resulted in a residual (R) of 7.87%. Anisotropic refinement of $LiMnSe_2$ showed reasonable thermal parameters and gave 5.10 and 10.44% for final $R(F)$ and $wR_2(F^2)$ with $I > 2\sigma(I)$. Because of the weak scattering power of Li, the position of Li in $LiMnSe_2$ was not determined. The largest remaining peak in the final Fourier difference map was 1.545 e/Å^3, located in the tetrahedral sites between the layers of the structure.

An orange platelike crystal of $NaMnSe_2$ with approximate dimensions $0.14 \times 0.11 \times 0.03$ mm was selected and mounted in a glass capillary. A full sphere ($\pm h, \pm k, \pm l$) of data with $5 \leq 2\theta \leq 60^\circ$ was collected. Of the reflections, 148 were unique and 143 with $I > 2\sigma(I)$ were used in the refinements. No systematic absences were observed. $NaMnSe_2$ is isostructural with $NaMnTe_2$ so the atomic positions of $NaMnTe_2$ were used to begin refinement (9). Isotropic refinement showed reasonable thermal coefficients for all atoms, and subsequent anisotropic refinement gave 4.74 and 9.37% for final $R(F)$ and $wR_2(F^2)$ with $I > 2\sigma(I)$. The largest remaining peak in the difference Fourier map was 1.889 e/Å^3 located in the tetrahedral holes between the layers.

An orange-red platelike crystal of $RbMnSe_2$ with approximate dimensions $0.20 \times 0.15 \times 0.05$ mm was selected and mounted in a glass capillary. A hemisphere ($+h, \pm k, \pm l$) of data with $5 \leq 2\theta \leq 60^\circ$ was collected. All data except those for which $h + k + l = 2n + 1$ were observed, consistent with a body-centered tetragonal space group. Of the reflections, 140 were unique and 136 with $I > 2\sigma(I)$ were used in the refinements. $RbMnSe_2$ in isostructural with the known phase $RbMnTe_2$, so the atomic positions of $RbMnTe_2$ were used to begin refinement (10). Isotropic refinement showed reasonable thermal coefficients for all atoms. Anisotropic refinement yielded 3.80 and 7.29% for final $R(F)$ and $wR_2(F^2)$ with $I > 2\sigma(I)$. The final difference Fourier map showed no residual density outside 1.972 and -2.151 e/Å^3.

$KMnSe_2$ and $CsMnSe_2$ are isostructural with $RbMnSe_2$; their cell parameters are determined and refined by Guinier X-ray diffraction patterns; $KMnSe_2$; $a = 4.2184(2)$ Å, $c = 13.767(1)$ Å, and $V = 244.98(2)$ Å^3; $CsMnSe_2$: $a = 4.3215(7)$ Å, $c = 14.473(2)$ Å, and $V = 270.29(7)$ Å^3.

An orange-red platelike crystal of $Na_2Mn_2Se_3$ with approximate dimensions $0.13 \times 0.07 \times 0.04$ mm was selected and mounted in a glass capillary. Indexing of Guinier X-ray powder patterns had established a monoclinic unit cell with lattice parameters, indicating that this phase was isostructural with a known compound, $Na_2Mn_2S_3$. A hemisphere ($+h, \pm k, \pm l$) of data with $5 \leq 2\theta \leq 55^\circ$ was collected. The systematic absences for hkl: $h + k \neq 2n$ and $h0l$: $l \neq 2n$ indicated $C2/c$ and Cc as possible space groups. It became clear that $Na_2Mn_2Se_3$ is isostructural with $Na_2Mn_2S_3$ ($C2/c$), and the atomic positions of $Na_2Mn_2S_3$ were used to begin the refinement (1). Of the reflections, 1635 were unique and 1588 were used in the refinements. Anisotropic refinement showed reasonable thermal parameters and gave 5.23 and 10.15% for final $R(F)$ and $wR_2(F^2)$ with $I > 2\sigma(I)$. The largest remaining peak and hole in the final Fourier difference map were 1.504 and -1.295 e/Å^3.

A summary of crystal and data collection parameters of $LiMnSe_2$, $NaMnSe_2$, $RbMnSe_2$, and $Na_2Mn_2Se_3$ are listed in Table 1, final atomic coordinates as shown in Table 2 and the anisotropic thermal parameters in Table 3.

DISCUSSION

Syntheses

We recently reported new ternary manganese tellurides, $AMnTe_2$ (A = Li, Na, K, Rb, Cs), $Na_3Mn_4Te_6$, and $NaMn_{1.56}Te_2$ (8–10). These ternary tellurides show many interesting structural types and interrelationships. Particularly interesting are the polar layers, $^2_\infty[MnTeTe_{3/3}]^-$, found in $AMnTe_2$ (A = Li, Na). Our attempts to prepare analogous selenides via direct and cation exchange reactions are discussed in this paper.

$LiMnSe_2$ was first synthesized using the stoichiometric proportions of starting materials Li, Mn, and Se in Nb tubes at 850°C for 7 days. Guinier X-ray powder patterns showed that the major products were Li_2Se and MnSe, but orange single crystals of $LiMnSe_2$ suitable for X-ray studies were obtained as a minor phase. After the structure and composition of $LiMnSe_2$ was determined, several reactions were

TABLE 1
Crystallographic Data for AMnSe$_2$ (A = Li, Na, Rb) and Na$_2$Mn$_2$Se$_3$

Empirical formula	$LiMnSe_2$	$NaMnSe_2$	$RbMnSe_2$	$Na_2Mn_2Se_3$
Crystal shape (color)	Plate (orange)	Plate (orange)	Plate (orange-red)	Plate (orange-red)
Crystal size (mm)	$0.13 \times 0.10 \times 0.05$	$0.14 \times 0.11 \times 0.03$	$0.20 \times 0.15 \times 0.05$	$0.13 \times 0.07 \times 0.04$
Space group, Z	$P3m1$ (No. 156), 1	$P3m1$ (No. 156), 1	$I\bar{4}m2$ (No. 119), 2	$C2/c$ (No. 15), 8
a, Å	4.1905(3)	4.2330(7)	4.2660(4)	15.689(2)
b, Å				13.888(2)
c, Å	6.6199(5)	6.9420(6)	14.033(2)	7.220(1)
β, deg				116.65(2)
V, Å^3	100.66(2)	107.72(4)	255.38(9)	1406.0(3)
Formula weight	219.80	235.85	298.33	392.74
T (°C)	20	20	20	20
λ (Å)	0.71073	0.71073	0.71073	0.71073
ρ_{calcd} (g/cm^3)	3.626	3.636	3.880	3.711
μ (mm^{-1})	21.104	19.826	26.110	19.119
$2\theta_{max}$, deg	55	60	60	55
h, k, l range	± 5, ± 5, ± 8	± 5, ± 5, ± 9	± 6, ± 6, ± 19	± 20, ± 15, ± 9
F(000)	96	104	260	1392
No. of obs. reflections	964	1042	827	3276
No. of unique reflections	115	148	140	1635
R_{int} (%)	5.24	6.38	5.99	9.54
Restraints/parameters	0/9	0/12	0/9	0/66
Goodness of fit	1.078	1.182	1.185	0.944
R_1,[a] wR_2[b] (%)	5.10, 10.44	4.74, 9.37	3.80, 7.29	5.03, 10.15
x and y in wR_2[b]	0.000, 5.086	0.051, 2.662	0.000, 9.768	0.011, 0.000
Flack parameter (x)	0.00	0.00	0.00	
Max., min. $\Delta\rho$, eÅ^{-3}	1.545, -1.882	1.889, -1.862	1.972, -2.151	1.504, -1.295

[a] $R_1(F) = \sum(|F_o| - |F_c|)/\sum(|F_o|)$.
[b] $wR_2(F^2) = [\sum|w(F_o^2 - F_c^2)^2|/\sum|w(F_o^2)^2|]^{1/2}$, $w = 1/[\sigma^2(F_o^2) + (xP)^2 + yP]$ where $P = (\text{Max}(F_o^2, 0) + 2F_c^2)/3$.

performed to find optimum reaction conditions for $LiMnSe_2$ formation.

The yield of $LiMnSe_2$ is highest when the reactants are Li, MnSe, and Se and the reaction is carried out at 950°C for 10 days with rapid quenching of the products. When the reactions were carried out below 950°C, the reaction products contain MnSe and Li_2Se as major products instead. When the reaction was followed with slow cooling, we observe the decomposition of $LiMnSe_2$ to from MnSe and Li_2Se. We observed that the formation of undesirable niobium selenides (Nb_3Se_4 and $NbSe_2$) was appreciably reduced when a binary starting material (MnSe) was used. It is likely that elemental Li and Se form less volatile and reactive Li_2Se_x ($x \leq 2$) early in the reaction. This is in contrast to the synthesis of $LiMnTe_2$ in which either elemental or binary starting materials can be used and slow cooling is recommended to obtain good single crystals. Silica tubes were used for the synthesis of $LiMnSe_2$ from the starting materials, Li_2Se, MnSe, and Se, but reaction products stuck to the silica tube and single crystals were not readily recovered. Furthermore, silica tubes are reactive to Li_2Se and sometimes do not survive the high reaction temperature (>950°C). Powder diffraction patterns indicate that among the products are $LiMnSe_2$ and MnSe, but the crystallinity of $LiMnSe_2$ was poorer than that obtained when a Nb container was used.

AMnSe$_2$ (A = Na, K, Rb, Cs) can be synthesized by loading $LiMnSe_2$, LiCl, and ACl in a 1:2:2 ratio at 850°C. The most likely driving fore for this type of reaction is the lattice energy difference between LiCl and ACl (A = K, Rb, Cs). This approach was used in the synthesis of $AMnTe_2$ (A = Na, K, Rb, Cs) from the corresponding $LiMnTe_2$ and AM_2Q_2 (A = Rb, Cs; M = Ni, Co; Q = S, Se) from the Tl compounds, TlM_2Q_2 (M = Ni, Co; Q = S, Se) (9, 10, 27). Unlike the telluride analogs, $AMnTe_2$ (A = Na, K, Rb, Cs), these newly synthesized selenides, AMnSe$_2$ (A = Na, K, Rb, Cs), are relatively stable in deoxygenated water for 2 or 3 days. Consequently, excess ACl and LiCl salts could be removed from selenides by washing with deoxygenated water and rinsing with acetone.

Attempts to synthesize $NaMnSe_2$ by loading elemental or binary starting materials in stoichiometric proportions at 750°C resulted in the formation of a mixture of $Na_2Mn_2Se_3$ and MnSe (see below). Subsequent attempts at the direct synthesis of $NaMnSe_2$ by changing reaction temperatures, loading compositions, and cooling speeds resulted in the formation of $Na_2Mn_2Se_3$ as a major phase, MnSe, and unidentified phases. Thus, neither $NaMnSe_2$ nor $NaMnTe_2$

TABLE 2
Atomic Coordinates and Equivalent Isotropic Displacement Parameters

Atom	Position	x	y	z	U_{eq}[a] (Å$^2 \times 10^3$)
			$LiMnSe_2$		
Mn	1*a*	0.0	0.0	0.6129(9)	18(1)
Se1	1*a*	0.0	0.0	0.0	15(1)
Se2	1*b*	1/3	2/3	0.4889(6)	16(1)
			$NaMnSe_2$		
Mn	1*a*	0.0	0.0	0.6258(8)	18(1)
Se1	1*a*	0.0	0.0	0.0	16(1)
Se2	1*b*	1/3	2/3	0.5133(7)	18(1)
Na	1*c*	2/3	1/3	0.260(2)	33(3)
			$RbMnSe_2$		
Rb	2*a*	0.0	0.0	0.0	23(1)
Mn	2*d*	0.0	0.5	3/4	10(1)
Se	4*e*	0.0	0.0	0.3521(1)	12(1)
			$Na_2Mn_2Se_3$		
Se1	8*f*	0.1452(1)	0.4242(1)	0.0655(2)	20(1)
Se2	8*f*	0.1335(1)	0.7202(1)	0.0498(2)	20(1)
Se3	8*f*	0.1113(1)	0.1139(1)	0.0483(2)	25(1)
Mn1	8*f*	0.2110(1)	0.5766(2)	0.2943(3)	22(1)
Mn2	8*f*	0.1857(2)	0.2621(2)	0.2610(4)	21(1)
Na1	4*e*	0.0	0.4298(8)	0.25	33(2)
Na2	4*e*	0.0	0.7203(6)	0.25	24(2)
Na3	8*f*	0.1018(5)	0.9155(5)	0.1310(9)	53(2)

[a] Equivalent isotropic U defined as $\frac{1}{3}$ of the trace of the orthogonalized U_{ij} tensor.

are readily synthesized by direct reactions. Attempts to synthesize $KMnSe_2$ by loading either elements or binaries as starting materials result in the formation of a mixture of K_2MnSe_2 and $KMnSe_2$, despite many attempts in which the loading composition, reaction time, and temperature were varied. $KMnSe_2$ was generally found as a minor product. Because the colors of K_2MnSe_2 and $KMnSe_2$ are similar (orange-red), it is impractical to physically separate $KMnSe_2$ from a reaction mixture. The indirect cation exchange method described above therefore proves to be the best means of obtaining pure $KMnSe_2$.

$Na_2Mn_2Se_3$ was first obtained in a reaction designed to synthesize $NaMnSe_2$ from elemental or binary starting materials. In several reactions intended to produce $Na_2Mn_2Se_3$, we observed that binary phases (MnSe and Na_2Se) were produced as major products at temperatures lower than 850°C. The same results are obtained when the silica tubes are used. Inspection of the Nb tube used as a container revealed clean and smooth surfaces, indicating no significant reaction with Se.

Despite many attempts involving variations of loading compositions, thermal treatments and reaction containers, the synthesis of ternary manganese selenides isostructural with $NaMn_{1.56}Te_2$ and $Na_3Mn_4Te_6$ (10) from either elemental or binary starting materials failed. These efforts inevitably yielded $Na_2Mn_2Se_3$ and Na_6MnSe_4 as the only ternary compounds formed.

$Na_2Mn_2Se_3$ and $LiMnSe_2$ are formed at high temperatures (>850°C) from elemental or binary starting materials in Nb or silica tubes. If appreciably lower temperatures are used, binary products, A_2Se (A = Li, Na) and MnSe, are observed. However, its synthesis requires quenching from above 850°C; only $LiMnSe_2$ seems to be genuinely unstable at these lower temperatures. $Na_2Mn_2Se_3$ is obtained in high yield when cooling from above 850° is slow.

Structure

The crystal structure of $NaMnSe_2$ is shown in Fig. 2, and selected interatomic distances and angles are listed in Table 4. $NaMnSe_2$ has polar layers, $^2_\infty[MnSeSe_{3/3}]^-$; half of the Se atoms (Se2) are bonded to three Mn atoms and the other half of Se atoms (Se1) are bound to only one Mn atom. In an alternative description, $MnSe_4$ tetrahedra are fused to give the intrinsic polarity of the extended layers by sharing Se atoms (Se2) in three corners. The $MnSe_4$ tetrahedra are so arranged that all the Mn–Se1 vectors point in the same direction (Se1 is the terminal Se atom; see Fig. 2).

TABLE 3
Anisotropic Thermal Parameters (Å$^2\times10^3$) for AMnSe$_2$ (A = Li, Na, Rb) and $Na_2Mn_2Se_3$

Atom	U_{11}	U_{22}	U_{33}	U_{12}	U_{13}	U_{23}
			$LiMnSe_2$			
Mn	16(1)	16(1)	22(2)	8(1)	0	0
Se1	14(1)	14(1)	16(2)	7(1)	0	0
Se2	16(1)	16(1)	16(2)	8(1)	0	0
			$NaMnSe_2$			
Na	35(5)	35(5)	29(7)	17(2)	0	0
Mn	15(1)	15(1)	23(2)	7(1)	0	0
Se1	12(1)	12(1)	23(2)	6(1)	0	0
Se2	18(1)	18(1)	18(1)	9(1)	0	0
			$RbMnSe_2$			
Rb	23(1)	23(1)	22(1)	0	0	0
Mn	8(1)	8(1)	16(2)	0	0	0
Se	17(1)	10(1)	10(1)	0	0	0
			$Na_2Mn_2Se_3$			
Se1	27(1)	16(1)	19(1)	−1(1)	13(1)	−1(1)
Se2	21(1)	22(1)	20(1)	−2(1)	12(1)	−2(1)
Se3	19(1)	19(1)	34(1)	0(1)	8(1)	−2(1)
Mn1	22(1)	23(1)	24(1)	0(1)	13(1)	−1(1)
Mn2	23(1)	19(1)	21(1)	2(1)	10(1)	1(1)
Na1	27(5)	37(6)	37(5)	0	16(4)	0
Na2	26(5)	22(5)	25(5)	0	13(4)	0
Na3	54(4)	21(4)	93(5)	4(4)	42(4)	10(5)

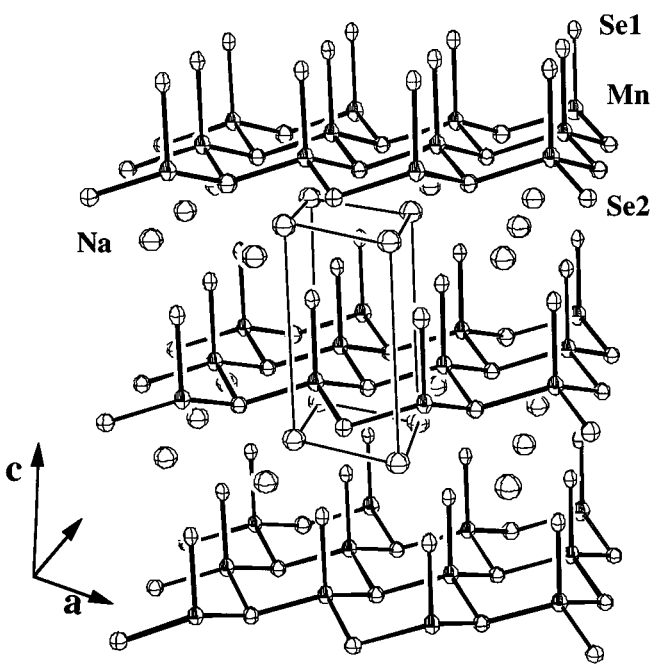

FIG. 2. Thermal ellipsoid plot of $NaMnSe_2$. 70% probability ellipsoids are shown.

X-ray studies show that $LiMnSe_2$ contains the same layered structure as that in $NaMnSe_2$, but the Li positions could not be determined. Our attempts to refine the Li positions were inconclusive. After Mn and Se atoms' locations and thermal parameters had been refined, peaks of comparable magnitude remained in both the octahedral and tetrahedral sites between the $[MnSe_2]^-$ layers. In $LiMnSe_2$, the Mn–Se1 bond distance (2.562(8) Å) is nearly identical to the other three Mn–Se2 bond distances (2.555(2) Å); for $NaMnSe_2$, the Mn–Se1 bond distance (2.597(6) Å) is slightly longer than the other three Mn–Se2 bond distances (2.566(2) Å). The Na^+ ions in $NaMnSe_2$ are in slightly irregular trigonal antiprismatic environments, having Na–Se distances $3 \times 3.04(1)$ Å (Se1) and $3 \times 3.01(1)$ Å (Se2). Oddly, both the Mn–Se and Na–Se distances are slightly longer for the four-coordinated selenium atoms (Se1) than for the six-coordinated selenium atoms (Se2). The shortest Se–Se contacts in $LiMnSe_2$ and $NaMnSe_2$ are 4.1905(3) and 4.2330(7) Å, respectively.

In the presence of larger alkali metal cations, *K*, Rb, and Cs, tetragonal $[MnSe_2]^-$ layers are formed by a symmetrical condensation of four-corner-shared tetrahedra, $[Mn_{4/4}Se_{4/2}]$. A thermal ellipsoid plot of $RbMnSe_2$ is shown in Fig. 3. Selected bond distances and angles for $RbMnSe_2$ are listed in Table 4. $[MnSe_2]^-$ layers are separated by alkali metals that center slightly compressed square prisms formed by eight Se atoms (Fig. 3). The distances between alkali metals and Se atoms in $RbMnSe_2$ are 3.662(1) Å (×8). Na atoms in $NaMnSe_2$ sit on the trigonal antiprismatic sites surrounded by six Se atoms, a difference that is clearly attributable to the increased size of the heavier alkali metal cations. The differences between the structures of the Li or Na compounds and the K, Rb, and Cs compounds are also seen in the telluride analogs (8–10). $RbMnSe_2$ layers consist of fairly regular $MnSe_4$ tetrahedra with Mn–Se distances of 2.569(1) Å (×4) and Se–Mn–Se angles of 108.10(3)° (×4) and 112.24(6)° (×2).

A polyhedral representation of the $Na_2Mn_2Se_3$ layer viewed on the *bc* plane and a thermal ellipsoid plot projected approximately along the *a* axis are shown in Fig. 4. Selected interatomic distances and angles are listed in Table 4. The structure consists of two hexagonally close-packed layers of Se atoms, between which 2/3 of the tetrahedral interstices filled to form zigzag chains. These chains are fused to form a two-dimensional layer by sharing other corners with each other (Fig. 4). As a result, networks comprise half of the tetrahedra that "point up" and half of the tetrahedra that "point down". The $MnSe_4$ tetrahedra are slightly distorted; Mn–Se bond distances in the

TABLE 4
Important Interatomic Distances (Å) and Angles (°)

	$LiMnSe_2$		
Mn–Sel	2.562(8)	Se1–Mn–Se2 (3×)	108.7(2)
Mn–Se2 (3×)	2.555(2)	Se2–Mn–Se2 (3×)	110.2(2)
	$NaMnSe_2$		
Mn–Se1	2.597(6)	Na–Se2 (3×)	3.01(1)
Mn–Se2 (3×)	2.566(2)	Na–Sel (3×)	3.04(1)
Sel–Mn–Se2 (3×)	107.7(1)	Se2–Mn–Se2 (3×)	111.2(1)
	$RbMnSe_2$		
Mn–Se (4×)	2.569(1)	Rb–Se (8×)	3.662(1)
Mn–Mn	4.266(1)	Se–Se	4.266(1)
Se–Mn–Se (4×)	108.10(3)	Se–Mn–Se (2×)	112.24(6)
	$Na_2Mn_2Se_3$		
Mn1–Se1	2.597(3)	Na1–Se1	3.113(2)
Mn1–Se1	2.590(3)	Na1–Se1(2×)	3.136(7)
Mn1–Se2	2.578(3)	Na1–Se1	3.113(2)
Mn1–Se3	2.548(3)	Na1–Se2 (2×)	3.057(7)
Mn1–Mn2	3.162(3)	Na2–Se1 (2×)	3.122(6)
Mn2–Se1	2.581(3)	Na2–Se2 (2×)	3.032(2)
Mn2–Se3	2.519(3)	Na2–Se3 (2×)	3.102(7)
Mn2–Se2	2.571(3)	Na3–Se2	2.865(8)
Mn2–Se2	2.602(3)	Na3–Se3	2.977(8)
Mn2–Mn2	3.138(5)	Na3–Se3	3.022(6)
Na2–Na3 (2×)	3.45(1)	Na3–Se3	2.837(8)
Se1–Mn1–Se1	108.3(1)	Se3–Mn2–Se2	110.1(1)
Se1–Mn1–Se2	105.32(9)	Se3–Mn2–Se1	116.5(1)
Se1–Mn1–Se3	119.5(1)	Se2–Mn2–Se1	105.7(1)
Se1–Mn1–Se2	107.2(1)	Se3–Mn2–Se2	103.6(1)
Se2–Mn1–Se3	103.5(1)	Se1–Mn2–Se2	115.2(1)
Se1–Mn1–Se3	113.0(1)	Se2–Mn2–Se2	105.3(9)

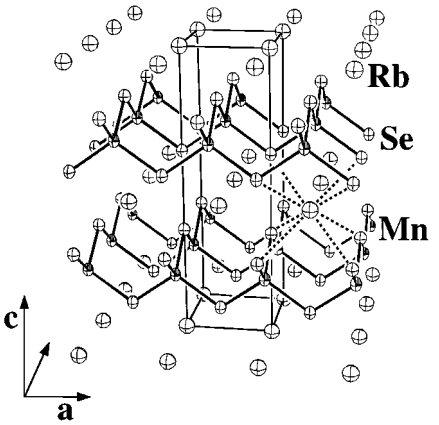

FIG. 3. Thermal ellipsoid plot of $RbMnSe_2$. 70% probability thermal ellipsoids are shown. Rb–Se contacts for one Rb atom are indicated with dashed lines.

tetrahedra fall between 2.548(3) and 2.602(3) Å, Se–Mn–Se angles range from 103.5(1) to 119.5(1)°. There are three crystallographically distinct Se atoms in the $Na_2Mn_2Se_3$; Se1 and Se2 are bonded to three Mn atoms in different ways but Se3 is bonded to two Mn atoms (Fig. 4; $^2_\infty[Mn_2Se_3] = {}^2_\infty[MnSe_{3/3}Se_{1/2}]$).

Sodium ions occupy $\frac{2}{3}$ of the octahedral sites (Na1 and Na2) and $\frac{1}{3}$ of irregular tetrahedral sites (Na3) between layers (see Fig. 4). The Na–Se distances in $Na_2Mn_2Se_3$ range from 2.837(8) to 3.136(7) Å.

Magnetic Measurements

The temperature-dependent molar magnetic susceptibilities and inverse molar magnetic susceptibilities for $AMnSe_2$ (A = Li, Na, K, Rb, Cs) and $Na_2Mn_2Se_3$ are shown in Fig. 5. On cooling, magnetic susceptibilities for $AMnSe_2$ (A = Li, Na) increase, reaching a maximum of 9 K, and then decrease. In Figs. 5a and 5b, we see that the inverse susceptibilities for $AMnSe_2$ (A = Li, Na) are linear above 120 K. These data were fit to a modified Curie–Weiss expression ($\chi = \chi_0 + N\mu_{eff}^2/(T-\theta)$, where χ_0 accounts for very small temperature-independent contributions that are handled imperfectly by our diamagnetic corrections, θ is the Weiss constant, μ_{eff} is the effective magnetic moment per Mn center, and N and k_B are Avogadro's and Boltzmann's constants), giving the following parameters: for $LiMnSe_2$, $\chi_0 = 1.70\times10^{-7}$ emu/mol, $\theta \cong -640$ K, and $\mu_{eff} = 4.68\,\mu_B$; for $NaMnSe_2$, $\chi_0 = 2.33\times10^{-5}$ emu/mol, $\theta \cong -1000$ K, and $\mu_{eff} = 4.79\,\mu_B$. The effective magnetic moments are nearly to 4.90 μ_B ($S = 2$), expected for a free high-spin Mn^{III} ion in a tetrahedral field. It is not clear that the decrease of magnetic susceptibilities of $AMnSe_2$ (A = Li, Na) around 9 K is caused by the antiferromagnetic transitions, but the large negative values of the Weiss constant (−640 and −1000 K) for these compounds indicate strong antiferromagnetic interactions between Mn^{III} ions.

The inverse susceptibility if $Na_2Mn_2Se_3$ increases on cooling and is linear above 70 K, giving $\chi_0 = 6.32\times10^{-4}$ emu/mol, $\theta \cong -140$ K, and $\mu_{eff} = 5.53\,\mu_B$. The effective moment is somewhat less than 5.92 μ_B ($S = \frac{5}{2}$), expected for a free high-spin Mn^{II} ion in a tetrahedral field. The corresponding sulfide, $Na_2Mn_2S_3$, which shows a nearly temperature-independent magnetic susceptibility over 4–300 K (1). Although no sharp antiferromagnetic transitions are observed, the negative value of the Weiss constant (−140 K) for $Na_2Mn_2Se_3$ implicates strongly interacting moments.

Sharp antiferromagnetic transitions were observed in the $AMnSe_2$ (A = K, Rb, Cs) series. These transitions are seen at 24 K for $KMnSe_2$, 10 K for $RbMnSe_2$, and 27 K for $CsMnSe_2$ (Figs. 5c and 5d). These compounds' reciprocal magnetic susceptibilities show nearly linear temperature

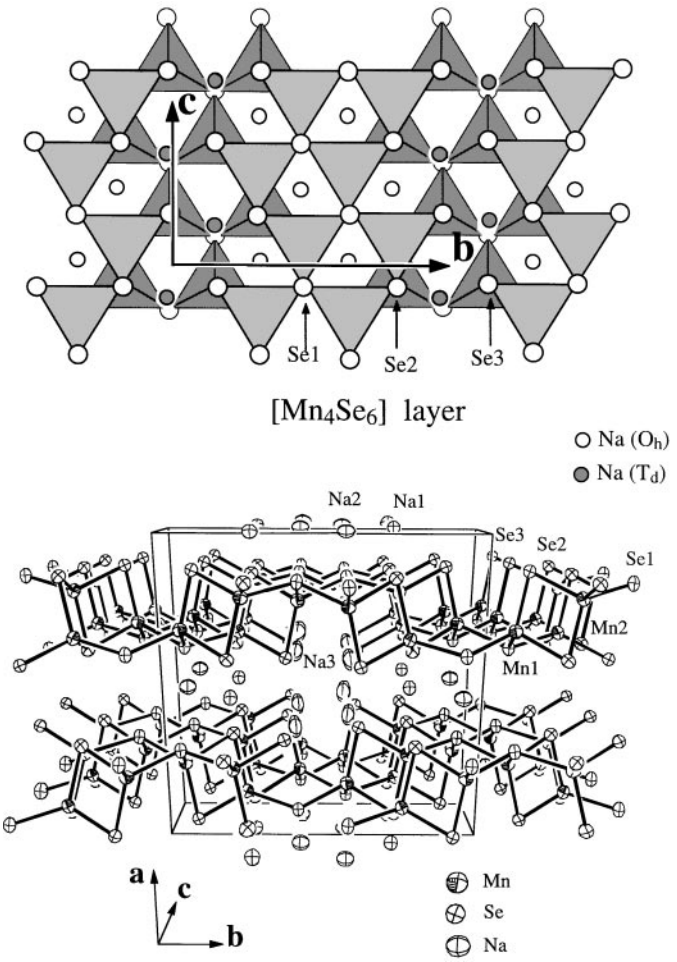

FIG. 4. Top: polyhedral representation of a $[Mn_2Se_3]^{2-}$ layer viewed on the bc plane. $MnSe_4$ tetrahedra are shown; Se atoms are indicated with open circles. Bottom: thermal ellipsoid (70% probability) plot of $Na_2Mn_2Se_3$ viewed down the c axis. Na atoms within the unit cell are shown.

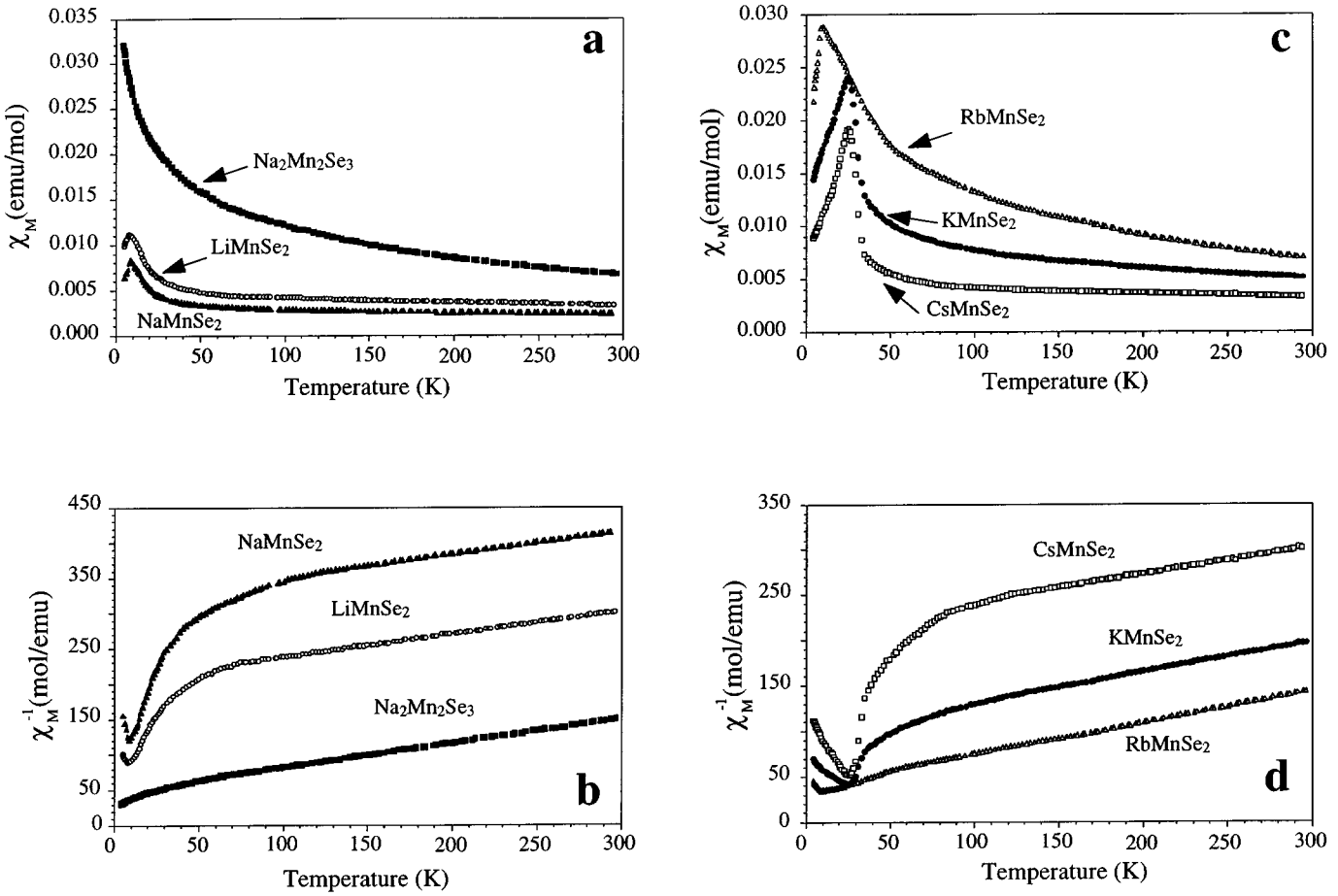

FIG. 5. Molar magnetic susceptibilities (a, c) and inverse molar susceptibilities (b, d) of $A\mathrm{MnSe_2}$ (A = Li, Na, K, Rb, Cs) and $\mathrm{Na_2Mn_2Se_3}$.

variation at higher temperatures. For $T > 80$ K, Curie–Weiss fits yielded the following parameters: for $\mathrm{KMnSe_2}$, $\chi_0 = 1.26 \times 10^{-6}$ emu/mol, $\theta \cong -280$ K, and $\mu_{\mathrm{eff}} = 4.84\ \mu_B$; for $\mathrm{RbMnSe_2}$, $\chi_0 = 1.79 \times 10^{-5}$ emu/mol, $\theta \cong -120$ K; and $\mu_{\mathrm{eff}} = 4.79\ \mu_B$; for $\mathrm{CsMnSe_2}$, $\chi_0 = 1.36 \times 10^{-6}$ emu/mol, $\theta \cong -680$ K, and $\mu_{\mathrm{eff}} = 5.06\ \mu_B$. The effective magnetic moments are in reasonable agreement with the value of 4.90 μ_B ($S = 2$), expected for a free high-spin Mn^{III} ion.

These results are comparable to those of telluride analogs and other manganese chalcogenides with two-dimensional nets of Mn atoms such as $A_2\mathrm{Mn_3}Q_4$ (A = Rb, Cs; Q = Se, Te) (6). Neutron studies of these compounds revealed that Mn spins were antiferromagnetically arranged within the layers. More extensive magnetic studies of the materials reported here are clearly needed.

CONCLUSIONS

The layered compounds, $A\mathrm{MnSe_2}$ (A = Li, Na, K, Rb, Cs) and $\mathrm{Na_2Mn_2Se_3}$, have been prepared and characterized by the use of single-crystal and powder X-ray diffraction, microprobe analysis, atomic absorption spectroscopy, and temperature-dependent magnetic studies. The proper choice of reaction conditions (temperature, cooling speed, reaction vessel, starting materials,. and their stoichiometry) are important for successful syntheses. All these compounds form layered structures with the $\mathrm{MnSe_4}$ tetrahedron as the fundamental building block. All compounds behave as nonideal Curie–Weiss paramagnets. Antiferromagnetic transitions are observed in $A\mathrm{MnSe_2}$ (A = K, Rb, Cs).

ACKNOWLEDGMENTS

This research was generously supported by the Texas Advanced Research Program through Grant 010366-097 and the National Science Foundation through Grant DMR-9215890. The R3m/V single-crystal X-ray diffractometer and crystallographic computing system were purchased from funds provided by the National Science Foundation (Grant CHE-8513273). We thank Dr. Renald Guillemette, Dr. Anatoly Bortun, and Mr. Aaron Dumar for their assistance with the microprobe analyses, atomic absorption measurements, and magnetic susceptibility measurements.

REFERENCES

1. K. Klepp, P. Böttcher, and W. Bronger, *J. Solid State Chem.* **47,** 301 (1983).
2. W. Bronger, U. Hendriks, and P. Müller, *Z. Anorg. Allg. Chem.* **559,** 95 (1988).
3. W. Bronger and H. Balk-Hardtdegen, *Z. Anorg. Allg. Chem.* **574,** 89–98 (1989).
4. W. Bronger, H. Balk-Hardtdegen, and D. Schmitz, *Z. Anorg. Allg. Chem.* **574,** 99 (1989).
5. W. Bronger and B. Bonsmann, *Z. Anorg. Allg. Chem.* **621,** 2083 (1995).
6. W. Bronger, H. Hardtdegen, M. Kanert, and D. Schmitz, *Z. Anorg. Allg. Chem.* **622,** 313 (1996).
7. E. J. Wu and J. A. Ibers, *Acta Crystallogr. Sect. C* **53,** 993 (1997).
8. C. Wang, J. Kim, and T. Hughbanks, *in* "Materials Research Society Symposium Proceedings," (A. Jacobson, P. Davies, T. Vanderah, and C. Torardi, C., Eds.), pp. 23–28. Materials Research Society, Boston, MA, 1997.
9. J. Kim, C. Wang, and T. Hughbanks, *Inorg. Chem.* **37,** 1428–1429 (1998).
10. J. Kim, C. Wang, and T. Hughbanks, *Inorg. Chem.* **38,** 235–242 (1999).
11. S. R. Marder, J. E. Sohn, and G. D. Stucky, *in* "Materials for Nonlinear Optics," (S. R. Marder, J. E. Sohn, and G. D. Stucky, Eds.), pp. 2–30, ACS Symposium Series 455. American Chemical Society, Washington, DC, 1991.
12. D. J. Williams, *Angew. Chem., Int. Ed. Engl.* **23,** 690 (1984).
13. R. T. Bailey, F. R. Cruickshank, P. Pavlides, D. Pugh, and J. N. Sherwood, *J. Phys. D: Appl. Phys.* **24,** 135 (1991).
14. J. Zyss and J. L. Oudar, *Phys. Rev. A* **26,** 2028 (1982).
15. D. F. Eaton, *Science* **253,** 281 (1991).
16. P. N. Prasad, *in* "Nonlinear Optical Materials," (G. Khanariam, Ed.) Proc. SPIE Vol. 1017, pp. 2–9, SPIE, Bellingham, WA, 1989.
17. P. G. Lacroix, R. Clément, K. Nakatani, J. Zyss, and I. Ledoux, *Science* **263,** 658 (1994).
18. R. Clément, L. Lomas, and J. P. Audière, *Chem. Mater.* **2,** 641 (1990).
19. R. Brec, *Solid State Ionics* **22,** 3 (1986).
20. A. Léaustic, J. P. Audière, P. Lacroix, R. Clément, L. Lomas, A. Michalowicz, W. R. Dunham, and A. H. Francis, *Chem. Mater.* **7,** 1103 (1995).
21. A. Léaustic, J. P. Audière, D. Cointereau, R. Clément, L. Lomas, F. Varret, and H. Constant-Machado, *Chem. Mater.* **8,** 1954 (1996).
22. F. Feher, *in* "Handbuck der Preparativen Anorganischen Chemie," (G. Brauer, Ed.) Ferdinand Enke Verlag, Stuttgart, Germany, 1954.
23. W. Klemm, H. Sodomann, and P. Langmesser, *Z. Anorg. Allg. Chem.* **241,** 281 (1939).
24. H. Franzen and C. Sterner, *J. Solid State Chem.* **25,** 227 (1978).
25. L. N. Mulay, *in* 'Theory and Applications of Molecular Diamagnetism," (L. N. Mulay and E. A. Boudreaux, Eds.), pp 289–307. Wiley-Interscience, New York, 1976.
26. G. M. Sheldrick, "SHELXTL-93 User Guide," Crystallography Department, University of Göttingen, Germany, 1993.
27. G. Huan, M. Greenblatt, and M. Croft, *Eur. J. Solid State Inorg. Chem.* **26,** 193 (1989).